Reversible Activation of a Cell-Penetrating Peptide in a Membrane Environment

ARTICLE *in* JOURNAL OF THE AMERICAN CHEMICAL SOCIETY · SEPTEMBER 2015

Impact Factor: 12.11 · DOI: 10.1021/jacs.5b06720

6 AUTHORS, INCLUDING:

Denise Schach

University of Chicago

18 PUBLICATIONS **108** CITATIONS

SEE PROFILE

Mischa Bonn

Max Planck Institute for Polymer Research

347 PUBLICATIONS **7,455** CITATIONS

SEE PROFILE

Sapun Parekh

Max Planck Institute for Polymer Research

39 PUBLICATIONS **882** CITATIONS

SEE PROFILE

Tobias Weidner

Max Planck Institute for Polymer Research

86 PUBLICATIONS **1,334** CITATIONS

SEE PROFILE

JACS
JOURNAL OF THE AMERICAN CHEMICAL SOCIETY
Communication
pubs.acs.org/JACS

Reversible Activation of a Cell-Penetrating Peptide in a Membrane Environment

Denise K. Schach,[‡] William Rock,[‡] Johannes Franz,[‡] Mischa Bonn, Sapun H. Parekh,* and Tobias Weidner*

Department of Molecular Spectroscopy, Max Planck Institute for Polymer Research, Mainz 55128, Germany

Supporting Information

ABSTRACT: Cell-penetrating peptides (CPPs) are promising molecules as drug carriers. However, because their uptake mainly involves endocytic mechanisms, endosomal trapping of the carrier (and drug) remains a high barrier for biomedical applications. The viral fusion mimic GALA, a pH-triggered CPP, takes advantage of the decreasing pH during endosome maturation to selectively attack endosomal membranes. Below pH 6, the sequence folds into a helix and can disrupt membranes. In this study, we show that the lipid bilayer radius-of-curvature has a negligible effect on GALA-induced leakage kinetics and that GALA remains pH responsive after inserting into a lipid membrane. The peptide can be reversibly "switched" between its inactive and active states after incorporation into the hydrophobic environment of lipid membranes, even after substantially interacting with lipid chains. This ability makes GALA-based delivery a potentially safe and efficient strategy for endosomal escape.

The fundamental barrier to successful drug delivery is moving cargo molecules across biomembranes. Many translocation strategies use specific (or nonspecific) endocytic pathways. However, endosomal trapping after initial cellular uptake is a major technical limitation for this drug delivery approach. A possible solution for this challenge is provided by pH-driven cell-penetrating peptides (CPPs), typically mimics of viral fusion machinery and antimicrobial peptides.[1] Besides endosomal escape, pH-triggered cell-penetration is promising for targeting cancer cells, which typically maintain lower pH conditions compared with healthy cells.[1b,2] One of the most studied representatives of this category is the EALA-repetition peptide GALA (sequence WEAALAEALAEALAEHLAEALAEALEALAA).[1a,3]

GALA assumes a random coil or α-helical structure, depending on the pH of the environment: At pH < 6, GALA adopts α-helical secondary structure. In its helical state, GALA can insert into membranes and has been shown to cause membrane leakage in unilamellar vesicles that are similar in size to endocytic vesicles.[4] At pH > 6, the glutamic acid side chains deprotonate and become negatively charged and consequently destabilize the helix structure (Scheme 1). In this unfolded state, the sequence is membrane inactive; it is "switched off".[3b] According to the current model, GALA can oligomerize within the membrane to form transmembrane pores of 10−12 monomers when "switched on".[3b,4] Indeed, GALA has been shown to target lipid membranes under slightly acidic ambient conditions *ex situ* and *in vitro*.[3b,5]

Scheme 1. Reversible Folding and Unfolding of GALA Peptides Is Triggered by the Protonation State of the Glutamic Acid Sites

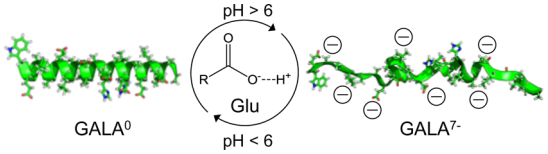

While phenomenological verification of pH-triggered GALA activity exists, the molecular behavior of GALA upon incorporation into the hydrophobic core of a lipid layer is still unclear. For drug delivery applications the most important questions are: (i) Does GALA activity depend on the membrane geometry and (ii) Is GALA still active, and can it therefore be 'switched off' at pH > 6, after membrane insertion? If the mechanism of GALA leakage depends on membrane geometry, then disruption of differently sized endosomes will have differential efficiency, and this has not been verified in model systems. Furthermore, disruption of cellular plasma membranes may prove to be challenging with GALA-linked molecular cargoes. The ability to switch GALA off is necessary to reduce unintended behaviors such as membrane fusion and potential secondary membrane disruption within cells. Both questions are important to understand the ultimate efficiency and safety of GALA-assisted drug delivery.

We recently reported that the functionality of GALA was suppressed when nonspecifically bound to the hydrophobic air−water surface; whereas, when attached to a hydrophilic gold surface via a terminal cysteine residue, GALA remained fully functional.[6] In view of this sensitivity to interfacial binding conditions, it is unclear whether GALA, once associated with the hydrophobic membrane core, still responds to pH changes in the surrounding aqueous media. This lack of fundamental physical-chemical understanding represents a challenge for rationally designing GALA-based systems for drug delivery.

GALA-induced pore formation and leakage has been studied extensively using unilamellar vesicles with diameters around 100 nm made of phosphocholine (PC) lipids (large unilamellar vesicles, LUVs).[4] Here, we used sum frequency generation (SFG) vibrational spectroscopy to focus on the mechanism of

Received: June 29, 2015
Published: September 3, 2015

DOI: 10.1021/jacs.5b06720
J. Am. Chem. Soc. 2015, 137, 12199−12202

reversibly triggered interaction between GALA and lipid interfaces. SFG is exceptionally useful to study minute amounts of ordered molecular structures at an interface such as folded peptides and proteins and model lipid membranes.[7]

However, SFG typically uses flat lipid surfaces, with zero curvature to probe interfacial structure. Therefore, the question arises whether results from SFG will be comparable to the previous studies using high-curvature submicron-diameter LUVs. Cellular compartments can also exhibit highly variable local membrane curvature. To determine the effect of the membrane geometry on pH-dependent GALA function, we studied GALA-induced leakage in giant unilamellar PC vesicles (GUVs, ∼ 3−20 μm diameter), which are much larger than previously used LUVs and therefore have a significantly smaller radius of curvature.

We prepared 1-palmitoyl-2-oleoyl-*sn*-glycero-3-phosphocholine (POPC) vesicles containing fluorescent dye using electroformation and tethered the GUVs to flat-bottom 96-well plate substrates via a biotin−streptavidin linkage to stabilize the GUVs for observing GALA-induced effects immediately after GALA addition (see Supporting Information (SI), Figure S1, for details). Time-lapse images with 7.5 or 15 s intervals were acquired immediately after pipetting a 1 μM GALA solution at the respective pH into the well. Figure 1 shows the initial and final images of the 30 min time-lapse videos (for the full videos, see SI, Movies S1 and S2). The images show that GALA at pH 7 induces almost zero leakage while at pH 5, many of the vesicles leak. The decay of the fluorescence intensity inside 23 vesicles was extracted (Figure 1F) and averaged as shown in Figure 1E. The average curve has a time constant of 23 s, consistent with the time constant from previous LUV PC leakage experiments with a similar lipid:protein ratio (2000:1).[4] The time-lapse experiments show that GALA causes GUV leakage with similar kinetics as observed for much smaller LUVs, which is consistent with the same surface density of GALA pores independent of vesicle size and a pore functionality that is not dependent on membrane curvature. Previous work also predicted "all or nothing" leakage, which was directly confirmed in the present data via imaging separate vesicles. From the GUV:peptide size ratio, we can consider the GUV surfaces quasi planar. Therefore, this result allows us to conclude that reducing the curvature of a lipid surface has negligible impact on GALA's ability to permeabilize membranes in a pH-dependent manner, indicating that the mechanistic function of GALA is unaffected.

To investigate the two-state molecular switching behavior of GALA in a lipid environment, we followed GALA activity at a membrane interface using SFG spectroscopy. We chose a lipid monolayer at the air−water interface at a surface pressure on the order of a typical cellular tension as a biomimetic system. Supported lipid bilayers have been used very successfully for SFG studies[8] but have some considerable drawbacks such as asymmetric contacts and hydration of the bilayer leaflets[9] and undefined lateral tension. Truly unsupported lipid membranes, such as black lipid membranes, would be ideal but are difficult to probe with SFG because of the IR absorption within the surrounding water.

In this experiment, a trough was filled with 25 mL D_2O at pH < 5 containing 10 mM sodium phosphate. 1,2-dipalmitoyl-*sn*-glycero-3-phosphocholine (DPPC) dissolved in chloroform was spread on the surface of the fluid. We used surface pressure measurements to follow membrane physical state in response to pH changes in the subphase with GALA present. We note

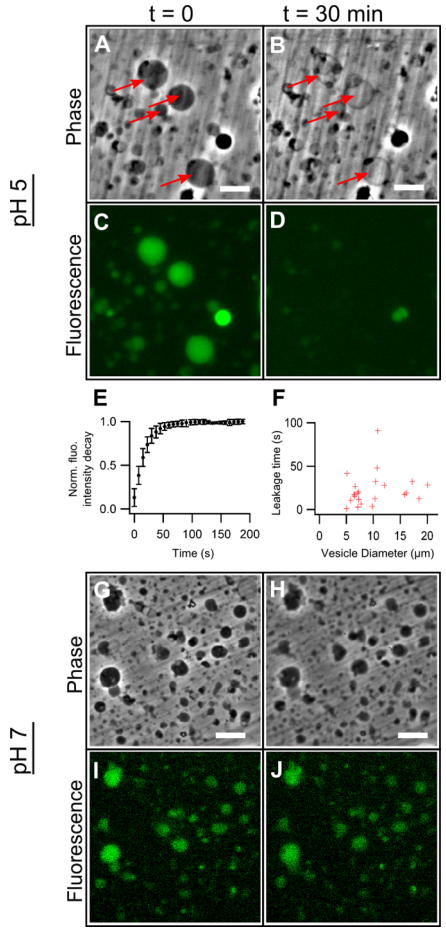

Figure 1. Time lapse experiment: GUVs at pH 5 (A−D) and 7 (G−J) immediately after GALA addition (left column: A,C,G,I) and after 30 min of incubation (right column: B,D,H,J). Leakage is only observed in the presence of GALA at pH 5 (arrows in A and B). The graphs between the images show the average fluorescence leakage kinetics from 23 different vesicles (E) and the histogram of leakage times vs size as determined by an exponential fit (F). The scale bar on all images is 20 μm and is the same for phase/fluorescence pairs (A/C, B/D, G/I, and H/J). Error bars in E are 95% confidence intervals.

that no agitation was used in the trough during these experiments in order to not perturb the sensitive structure of lipid monolayers. Therefore, we titrated extreme acidic and basic pH values far from the peptide's transition pH (pH 6) to avoid potential mixed states due to diffusive equilibration of pH. After spreading DPPC, a surface pressure between 20 and 25 mN/m provided a well-ordered, liquid-condensed model membrane (stage I, Figure 2A). The slight long-term decrease of surface pressure occurs due to the evaporation of D_2O.

SFG spectra in the ssp polarization combination at the water/lipid surface (Figure 2B) were recorded at the times indicated by the Roman numerals in Figure 2A. The SFG spectrum of the DPPC monolayer shows a peak at 1734 cm^{-1} that originates from the carbonyl stretch (C═O) vibration in phospholipids (stage I, Figure 2B). After 50 min, GALA (0.2 mg/50 μL, pH < 5) was injected into the subphase. The immediate increase in surface pressure of more than 10 mN/m (in the shape of a Langmuir adsorption kinetic) indicates GALA surface activity and incorporation into the lipid monolayer. The surface pressure saturates, and the corresponding SFG spectrum (stage II, Figure 2B) shows an amide I signal

DOI: 10.1021/jacs.5b06720
J. Am. Chem. Soc. 2015, 137, 12199−12202

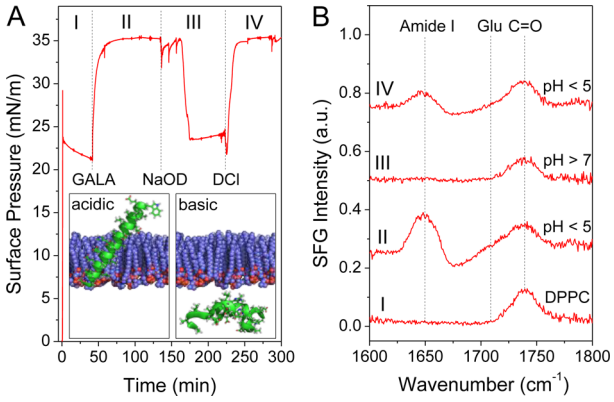

Figure 2. Switchable membrane insertion activity of GALA. (A) Surface pressure of a DPPC monolayer spread on an acidic aqueous solution before (I) and after (II) the addition of GALA into the subphase. Adjusting the pH to basic (III) or acidic (IV) conditions results in peptide expulsion or re-insertion, respectively. Schemes depict the inserted α-helical form of GALA (green) under acidic conditions and the inactive unordered form under basic conditions. (B) SFG spectra corresponding to stages I–IV. The DPPC monolayer in absence (I) and presence of the inactive peptide (III) only show a lipid stretch vibration at 1734 cm^{-1}. At low pH (II and IV), the active α-helical form of GALA shows a characteristic amide I signal at 1650 cm^{-1}. Spectra are offset for clarity.

at 1650 cm^{-1}. This vibration corresponds to the α-helical state of GALA. Also, a band centered around 1710 cm^{-1} appears, which can be assigned to the antisymmetric stretch vibration of the protonated glutamic acid side chains.[10] Next, the pH of the solution was increased to pH > 7 by the addition of NaOD, resulting in a subsequent drop in surface pressure during stage III (Figure 2A). The observed SFG spectrum is similar to that of the pure lipid monolayer, as no amide I (or band at 1710 cm^{-1}) signal was observed, while the carbonyl stretch vibration of the lipid remained.

While the transition of GALA to a disordered state[11] by raising the pH is directly apparent, by lack of an amide I vibration in the stage III SFG spectrum (also for ppp spectra, see SI, Figure S2), it remains possible that GALA is still present in the vicinity of the DPPC monolayer due to the selection rules for SFG spectroscopy. This is further supported by the persisting increase in surface pressure (compared to original surface pressure without peptide) even after addition of NaOD (Figure 2A, stage III). We surmise that the residual increase in surface pressure arises from the peptide weakly interacting with the zwitterionic DPPC lipid head groups. This view is supported by surface tension data recorded for the injection of GALA into an initially basic subphase (see SI, Figure S3). In analogy with the stage III discussed above, the data show a slight increase in surface pressure, also indicating that GALA associates with the lipid surface. Finally, the pH was decreased again to pH < 5 by adding DCl (stage IV, Figure 2A). The surface pressure increases again to the value of stage II (Figure 2A), and the SFG data (Figure 2B) of stage II and IV also look very similar. This demonstrates the reversibility of GALA insertion after pH cycling. We note, however, that it is not possible to distinguish between previously membrane bound species and dissolved species that insert into the lipid layer for the first time. The reversibility of surface pressure lets us assume that the lipid/inserted peptide ratio is comparable to that at stage II. We note that these experiments were additionally performed with POPC, a more fluid lipid, and showed identical results (see SI, Figure S4).

To glean information about how GALA affects the molecular order within a cell-like membrane, CD stretch vibrations of an isotopically labeled 1,2-dipalmitoyl-d62-*sn*-glycero-3-phosphocholine (d62-DPPC) monolayer were followed using SFG spectroscopy in a Langmuir trough in which the surface pressure was kept constant at 20 mN/m. A constant surface pressure experiment allows the membrane to expand upon GALA insertion and thus reflects the biological response of lipid molecules.[12] In Figure 3, ssp SFG spectra of a d62-DPPC

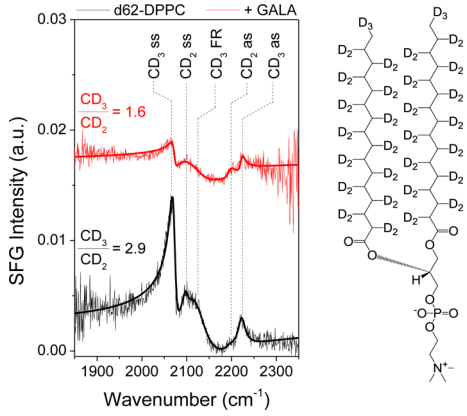

Figure 3. SFG spectra of model membrane perturbation upon GALA insertion. Due to the isotopically labeled acyl chains, the lipid monolayer gives deuterocarbon signals in the CD range that selectively reflect the molecular order in the hydrophobic region of the model membrane. SFG spectra show the lipid monolayer spread on an acidic aqueous subphase before (black) and after (red) the injection of GALA into the subphase (pH 5) at a fixed surface pressure of 20 mN/m. Overall signal intensity decreases as lipid density decreases due to membrane relaxation. The dramatically reduced CD_3/CD_2 ratio shows extensive membrane perturbation due to GALA insertion. Spectra are offset for clarity.

monolayer in the CD region are shown before (black) and after (red) the injection of GALA into an acidic aqueous subphase. SFG responses in the amide and CH region are shown in the SI (Figure S5). As only the acyl chains are isotopically labeled, Figure 3 reflects solely the hydrophobic deuterocarbon chains of the model membrane.

The spectra exhibit a dominant resonance near 2070 cm^{-1} assigned to the symmetric CD_3 stretching vibration. The spectra also display the antisymmetric CD_3, symmetric and antisymmetric CD_2, and the CD_3 Fermi resonance near 2225, 2100, 2200, and 2125 cm^{-1}, respectively. In the presence of active GALA the overall SFG intensity goes down as the surface density of lipids decreases due to the trough barrier moving to keep the surface pressure constant because of GALA's surface affinity. In addition, a strong decrease in the CD_3 intensities relative to CD_2 signals was observed. The methyl/methylene ratio is a convenient marker to quantify chain order in lipid layers.[13] The peak ratio decreases to about 55% (see SI, Table S1, for fitting results) in the presence of GALA, indicating a diminished acyl chain order and alignment in the model membrane when interacting with active GALA peptides.

To fully understand the molecular mechanisms by which GALA acts on lipid membranes, a series of detailed, spectroscopic studies to investigate the impact of GALA on different lipid chemistries (charge, mixtures, domains struc-

DOI: 10.1021/jacs.5b06720
J. Am. Chem. Soc. 2015, 137, 12199–12202

tures) and the effect of actual molecular cargoes or even drug particles on GALA activity will be important. This study provides a first step toward a more detailed understanding of fundamental GALA–lipid interactions. The results demonstrate that membrane curvature is not a critical parameter for activity, indicating that GALA does not have enhanced activity on specific cell membrane domains based on their local curvature alone. SFG data show that natural confinement of GALA, and possibly other pH-active viral fusion peptide mimics, within the hydrophobic environment of a lipid layer does not interfere with its reversible folding and membrane activity. This is particularly noteworthy in view of diminished reversibility of GALA folding observed at other hydrophobic interfaces and consequently for applications of the GALA sequence in safe bioengineered drug carrier systems. The results demonstrate the peptide can be deactivated upon exposure to the pH 7.4 cytosol after disrupting an endosome. This indicates that the pH-triggered GALA platform is a viable approach to imparting molecular cargoes and particle surfaces with reversible pH responsive membrane activity.

■ ASSOCIATED CONTENT

Supporting Information

The Supporting Information is available free of charge on the ACS Publications website at DOI: 10.1021/jacs.5b06720.

Experimental section; Figures S1–S5; Table S1(PDF)
Movie S1 (AVI)
Movie S2 (AVI)

■ AUTHOR INFORMATION

Corresponding Authors

*parekh@mpip-mainz.mpg.de
*weidner@mpip-mainz.mpg.de

Author Contributions

‡These authors contributed equally.

Notes

The authors declare no competing financial interest.

■ ACKNOWLEDGMENTS

This work was supported by grants from the Marie Curie Foundation: nos. CIG322284 (SHP) and CIG322124 (TW). J.F. and T.W. acknowledge funding from the Deutsche Forschungsgemeinschaft (WE4478/2-1).

■ REFERENCES

(1) (a) Erazo-Oliveras, A.; Muthukrishnan, N.; Baker, R.; Wang, T. Y.; Pellois, J. P. *Pharmaceuticals* **2012**, *5*, 1177–1209. (b) Lee, E. S.; Gao, Z. G.; Bae, Y. H. *J. Controlled Release* **2008**, *132*, 164–170.

(2) (a) Yamada, Y.; Shinohara, Y.; Kakudo, T.; Chaki, S.; Futaki, S.; Kamiya, H.; Harashima, H. *Int. J. Pharm.* **2005**, *303*, 1–7. (b) Yao, L.; Daniels, J.; Moshnikova, A.; Kuznetsov, S.; Ahmed, A.; Engelman, D. M.; Reshetnyak, Y. K.; Andreev, O. A. *Proc. Natl. Acad. Sci. U. S. A.* **2013**, *110*, 465–470. (c) Andreev, O. A.; Engelman, D. M.; Reshetnyak, Y. K. *Mol. Membr. Biol.* **2010**, *27*, 341–352. (d) Zoonens, M.; Reshetnyak, Y. K.; Engelman, D. M. *Biophys. J.* **2008**, *95*, 225–235.

(3) (a) Nishimura, Y.; Takeda, K.; Ezawa, R.; Ishii, J.; Ogino, C.; Kondo, A. *J. Nanobiotechnol.* **2014**, *12*, 11. (b) Li, W.; Nicol, F.; Szoka, F. C., Jr. *Adv. Drug Delivery Rev.* **2004**, *56*, 967–985.

(4) Parente, R. A.; Nir, S.; Szoka, F. C., Jr. *Biochemistry* **1990**, *29*, 8720–8728.

(5) Hatakeyama, H.; Ito, E.; Akita, H.; Oishi, M.; Nagasaki, Y.; Futaki, S.; Harashima, H. *J. Controlled Release* **2009**, *139*, 127–132.

(6) Schach, D.; Globisch, C.; Roeters, S. J.; Woutersen, S.; Fuchs, A.; Weiss, C. K.; Backus, E. H.; Landfester, K.; Bonn, M.; Peter, C.; Weidner, T. *J. Chem. Phys.* **2014**, *141*, 22D517.

(7) (a) Rzeznicka, I. I.; Pandey, R.; Schleeger, M.; Bonn, M.; Weidner, T. *Langmuir* **2014**, *30*, 7736–7744. (b) Chen, X.; Wang, J.; Kristalyn, C. B.; Chen, Z. *Biophys. J.* **2007**, *93*, 866–875. (c) Serebryany, E.; Zhu, G. A.; Yan, E. C. *Biochim. Biophys. Acta, Biomembr.* **2012**, *1818*, 225–233. (d) Fu, L.; Liu, J.; Yan, E. C. *J. Am. Chem. Soc.* **2011**, *133*, 8094–8097. (e) Nguyen, K. T.; King, J. T.; Chen, Z. *J. Phys. Chem. B* **2010**, *114*, 8291–8300. (f) Weidner, T.; Dubey, M.; Breen, N. F.; Ash, J.; Baio, J. E.; Jaye, C.; Fischer, D. A.; Drobny, G. P.; Castner, D. G. *J. Am. Chem. Soc.* **2012**, *134*, 8750–8753. (g) Weidner, T.; Breen, N. F.; Li, K.; Drobny, G. P.; Castner, D. G. *Proc. Natl. Acad. Sci. U. S. A.* **2010**, *107*, 13288–13293. (h) Weidner, T.; Castner, D. G. *Phys. Chem. Chem. Phys.* **2013**, *15*, 12516–12524.

(8) (a) Chen, X.; Wang, J.; Boughton, A. P.; Kristalyn, C. B.; Chen, Z. *J. Am. Chem. Soc.* **2007**, *129*, 1420–1427. (b) Ding, B.; Chen, Z. *J. Phys. Chem. B* **2012**, *116*, 2545–2552.

(9) Castellana, E. T.; Cremer, P. S. *Surf. Sci. Rep.* **2006**, *61*, 429–444.

(10) Barth, A. *Prog. Biophys. Mol. Biol.* **2000**, *74*, 141–173.

(11) Goormaghtigh, E.; De Meutter, J.; Szoka, F.; Cabiaux, V.; Parente, R. A.; Ruysschaert, J. M. *Eur. J. Biochem.* **1991**, *195*, 421–429.

(12) Janmey, P. A.; Kinnunen, P. K. *Trends Cell Biol.* **2006**, *16*, 538–546.

(13) Guyot-Sionnest, P.; Hunt, J. H.; Shen, Y. R. *Phys. Rev. Lett.* **1987**, *59*, 1597–1600.

DOI: 10.1021/jacs.5b06720
J. Am. Chem. Soc. 2015, 137, 12199–12202